AIR FORCE INSTITUTE OF TECHNOLOGY

AIR UNIVERSITY
UNITED STATES AIR FORCE

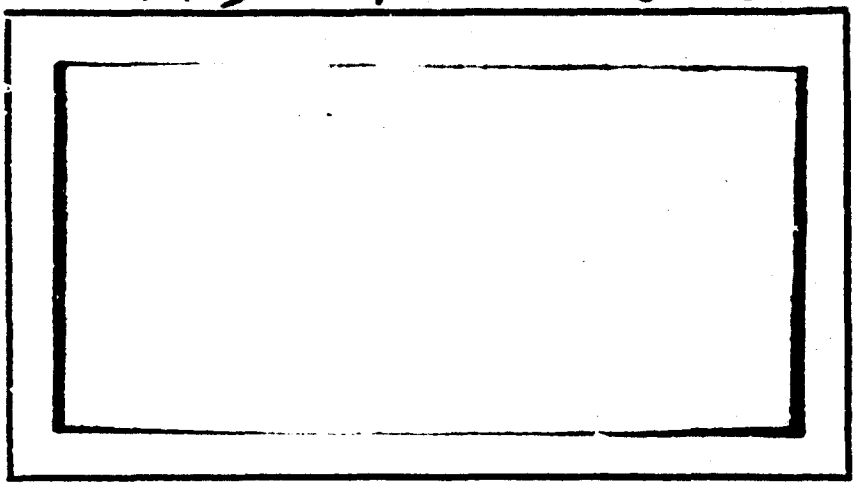

SCHOOL OF ENGINEERING

WRIGHT-PATTERSON AIR FORCE BASE, OHIO

EXPERIMENTAL STUDY OF

INSTABILITIES IN THE ELMAX

THESIS

GEP/PH/72-22 Victor R. Trouy
Captain USAF

I

Unclassified

Security Classification

DOCUMENT CONTROL DATA - R & D

(Security classification of title, body of abstract and indexing annotation must be entered when the overall report is classified)

1. ORIGINATING ACTIVITY (Corporate author)	2a. REPORT SECURITY CLASSIFICATION
Air Force Institute Of Technology (AFIT-EN) Wright-Patterson AFB, Ohio 45433	Unclassified
	2b. GROUP

3. REPORT TITLE

Experimental Study of Instabilities in the ELMAX

4. DESCRIPTIVE NOTES *(Type of report and inclusive dates)*

AFIT Thesis

5. AUTHOR(S) *(First name, middle initial, last name)*

Victor R. Trouy
Capt USAF

6. REPORT DATE	7a. TOTAL NO. OF PAGES	7b. NO. OF REFS
June 1972	49	13

8a. CONTRACT OR GRANT NO.	9a. ORIGINATOR'S REPORT NUMBER(S)
b. PROJECT NO. 7073-00-07	GEP/PH/72-22
c. DoD Element 61102F DoD Subelement 681301	9b. OTHER REPORT NO(S) *(Any other numbers that may be assigned this report)*

10. DISTRIBUTION STATEMENT

Approved for public release, distribution unlimited.

11. SUPPLEMENTARY NOTES	12. SPONSORING MILITARY ACTIVITY
	AFIT School of Engineering

13. ABSTRACT

An experimental search for instabilities in an ELMAX plasma device was made. Plasma generated oscillations of potential and density, with amplitudes several orders of magnitude above background noise, were observed over a wide range of plasma parameters. Measurements of plasma parameters were made with Langmuir probe diagnostic techniques. Frequencies from 3 kHz to 8 kHz were observed with phase velocity in the direction of the electron diagmagnetic drift. Ion temperature was not measured and attempted measurements of space potential were not satisfactory. By comparing the observed characteristics of the oscillations with previously identified instabilities, the instabilities responsible for the plasma generated oscillations were tentatively identified as collisional drift waves.

11

DD FORM 1 NOV 68 1473

Unclassified

Security Classification

14. KEY WORDS	LINK A		LINK B		LINK C	
	ROLE	WT	ROLE	WT	ROLE	WT
Plasma Instabilities						
Magnetic Mirror						
Plasma Containment						
Drift Instabilities						

EXPERIMENTAL STUDY OF INSTABILITIES IN THE ELMAX

THESIS

Presented to the Faculty of the School of Engineering

of the Air Force Institute of Technology

Air University

in Partial Fulfillment of the

Requirements for the Degree of

Master of Science

by

Victor R. Trouy, B.S.

Captain USAF

Graduate Engineering Physics

June 1972

Preface

This study is the result of my attempts to experimentally locate instabilities in the ELMAX plasma device. I was fortunate to be given a sophisticated and well designed research tool already in operation. With the exceptions of a few leak-hunts in the vacuum system and the contruction of a few probes, no time was used in preparing equipment for the experiment.

Since preparing the equipment was not a part of the study, the equipment and data acquisition system are only briefly described in this paper.

My grateful thanks go to Dr. Gordon Soper, for his patient endurance throughout this study, and to Major Justin Curtis and Drs. John Martin and Merrill Andrews for their many suggestions and hours of assistance.

Many thanks also to Mr. Cliff Van Sickle, Mr. Dennis Grossjean and Mr. Bill Cadwallender, without whom the sophisticated research would never have functioned.

Victor R. Trouy

Contents

GEP/PH/72-22

Abstract

An experimental search for instabilities in an ELMAX plasma device was made. Plasma generated oscillations of potential and density, with amplitudes several orders of magnitude above background noise, were observed over a wide range of plasma parameters. Measurements of plasma parameters were made with Langmuir probe diagnostic techniques. Frequencies from 3 kHz to 8 kHz were observed with phase velocity in the direction of the electron diamagnetic drift. Ion temperature was not measured and attempted measurements of space potential were not satisfactory. By comparing the observed charactertistics of the oscillations with previously identified instabilities, the instabilities responsible for the plasma generated oscillations were tentatively identified as collisional drift waves.

I. Introduction

The Electrodynamic Magnetoplasma Experiment (ELMAX) is designed to achieve improved plasma containment in a magnetic mirror device. To reduce microinstabilities, an external electric field is applied, and careful design of the plasma injection devices is intended to provide a nearly Maxwellian particle distribution. The remaining instabilities are expected to be macroscopic in nature and therefore susceptible to feedback stabilization. In order to explore the feasability of feedback stabilization, it was first necessary to determine what instabilities were present in the plasma, and that was the purpose of this study.

Langmuir-probe diagnostic techniques were used to study the plasma. The probe outputs were used as inputs to a spectrum analyzer, an oscilloscope, and a computer analysis system developed by Nunn (Ref 1). A description of the apparatus is given in Section II, and the experimental procedures used are described in Section III.

Since probe theory in a magnetic field is still not completely developed, the results of the computer analysis are open to some question. However, the results proved to be very repeatable and throughout this study they are assumed to be correct. The one exception to this is the measured space potential. As explained in Section III, attempts to use the gradient of space potential to determine the electric field gave ambiguous results. Another important parameter

which was not available during this study was the ion temperature. Although an ion probe had been designed and was being built, it was not available during this study. The lack of these two important parameters made identification of the observed instabilities more difficult and less certain. In particular, it was found that precise knowledge of the electric field would permit one to distinguish the differences between a flute instability and a drift instability. This was particularly significant since the observed instabilities exhibited characteristics common to both.

Another limitation imposed by the apparatus was the frequency range over which measurements were made. Because of high-frequency attenuation in the data-collecting circuits, no attempt was made to observe frequencies above 100 kHz. This limitation is not a severe one since the most useful frequencies for initial experiments with feedback stabilization are lower than 100 kHz.

Section IV includes a comparison of experimental results with theory. If the drift caused by the electric field is assumed to be negligible, it is shown that all of the observed characteristics of the instability conform to those of a drift wave, and that the stability conditions for a drift wave correctly predict the stability of the observed oscillations.

II. Experimental Apparatus

Vacuum System

The plasma was produced in a cylindrical vacuum chamber with an internal diameter of 23.5 in. and an internal length of 22.68 in. The chamber had three 7.8 in.-diameter ports in the median plane spaced 90 degrees apart with one centered on the top of the chamber and two on the sides. One side port was used with a quartz window to allow visual observation of the plasma. There were 18 radial ports near each end of the chamber, spaced at 20 degree intervals, approximately 8.5 in. on either side of the median plane. The chamber and other important components of the experimental apparatus are sketched in Fig. 1. The vacuum system included a 10-in. CVC diffusion pump, a liquid-nitrogen-cooled baffle, one 50 cfm and one 12 cfm roughing pump, and pneumatic valves to control the system. Base pressures of 2×10^{-7} torr are obtained using the baffle and 6×10^{-6} torr without the baffle.

Magnets

As shown in Fig. 1, two magnet coils were mounted at each end of the chamber. The two inboard magnets are 4-in.-thick, 248 turn Magnion coils. They are mounted next to the end of the chamber flange with their centers 38.60 ± .05 cm from the median plane. The two outboard magnets were 5-in.-thick, 122-turn Magnion coils and were mounted with their centers 63.10 ± .05 cm from the median plane. The geometric centers of

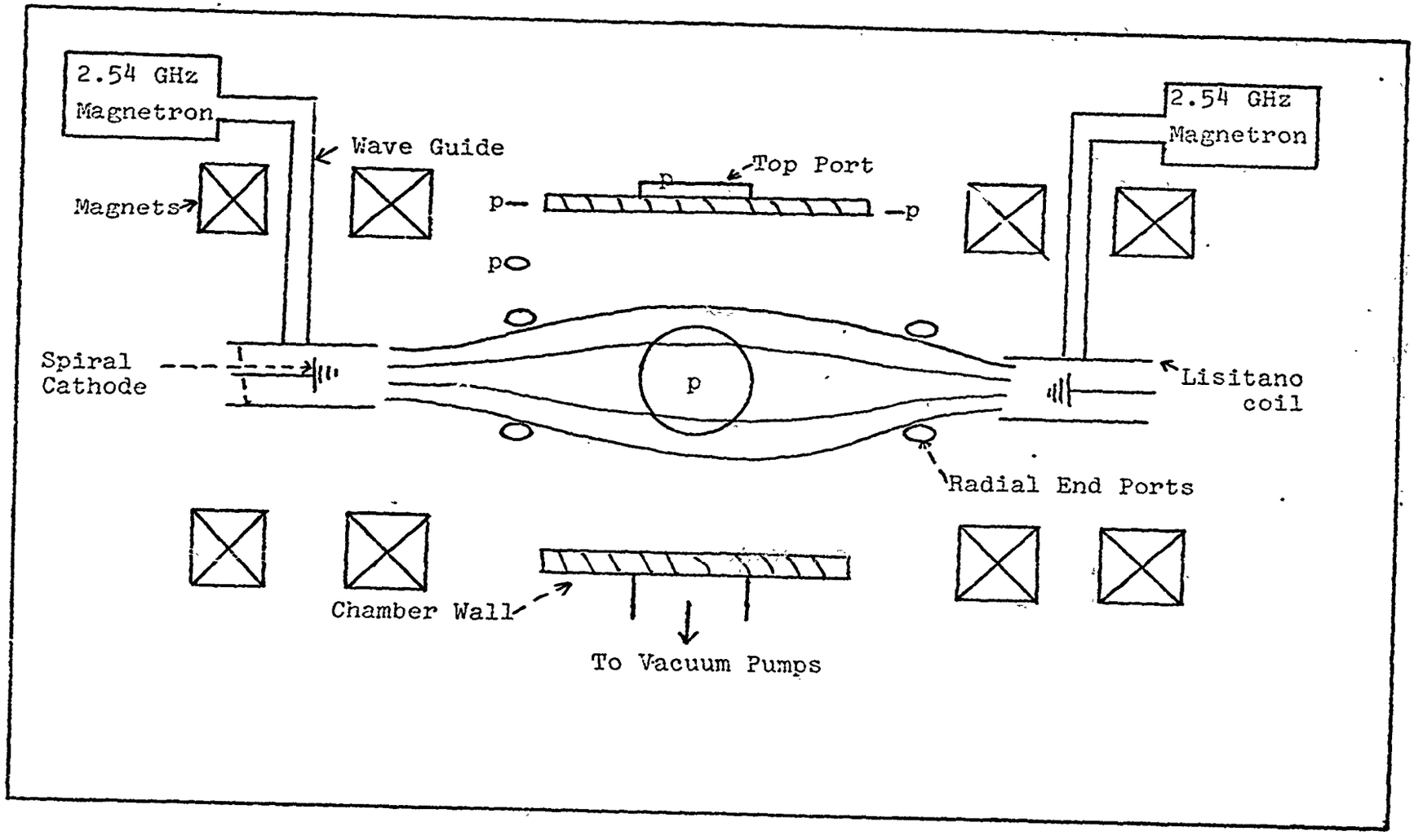

Fig. 1. The ELMAX Chamber

the coils were aligned to within ± 0.05 cm of the chamber axis. The power supplies were able to provide 250 amps of current to the outboard magnets which were wired in series, and 200 amps total current to the inboard magnets which were wired in parallel. This provided a magnetic field in the chamber of approximately 450 gauss at the chamber axis near the end probes (8.5 in. axially from the median plane) and approximately 235 gauss on axis at the median plane. The maximum magnetic field, occuring at each end of the chamber, is approximately four times the field at the median plane, resulting in a mirror ratio of four to one. At the plasma pressures observed throughout this study, the ratio of plasma pressure to magnetic pressure is very low (Beta much less than one) and the applied magnetic field is assumed to be unchanged by the presence of the plasma.

Lisitano Coils and Spiral Cathodes

The plasma sources, located at each end of the chamber between the inboard and outboard magnets, consisted of a 4-in. diameter helical Lisitano coil with a 3.5 in. i. d. quartz liner, and a 2 in. diameter heated spiral. The microwave source for each Lisitano coil was a 1 kw, 2.45 GHz air-cooled magnetron r.f. generator. Both magnetrons were powered by the same 4 kw, 500mA d.c. power supply. The magnetrons were connected to the coils through a wave guide and stub tuner. Each Lisitano coil consisted of a hollow metal cylinder with a continuous slot machined through the cylinder wall in the shape of a helix. The slot served as a transmission line for

the power from the magnetrons, and the net effect was an oscillating electric field applied to the plasma. The direction of the electric field was made to be almost parallel to the applied magnetic field by using coils with small helix angles. The d.c. power supplies for the spiral cathodes supplied approximately 28 volts at 90 amps to the spirals. The polarity of the voltage could be reversed, and the spirals could be operated with either end grounded or with both ends floating. Changing the grounding of the spirals was found to have no useful effect on the plasma but reversing the polarity of the voltage resulted in a reversal of the applied radial electric field. In the experiments described in this study, the voltage is applied to the spirals so that the radial field is directed inward toward the center of the plasma. An electric field pointing outward was found to result in a hollow plasma with maximum density near the outer edge of the spirals rather than on the axis of the chamber.

Langmuir Probes

Two radially traversing, Langmuir, single probes at right angles to one another were mounted in the median plane of the chamber. Two other probes were mounted in two of the radial end ports, one on top of the chamber in line with the top center probe, and the second in a side port, 40 degrees from the first. Occasionally, one of the end probes was moved to the top end port at the other end of the chamber to make measurements. This allowed the symmetry of the plasma along

the axis of the chamber to be measured, and also allowed simultaneous observation of any observed oscillations at both ends and at the center of the chamber. This provided information about the volume of the plasma affected by the oscillation and the phase relation of the oscillation at one end of the chamber relative to the center or other end of the chamber. The ports in which probes were installed are marked in Fig. 1 with a "p".

Data Collecting Equipment

To observe and record data directly from the various probes, a dual-beam Tektronix oscilloscope, type 551, was used with two plug-in units, a Nelson Ross spectrum analyzer with a range from 0 to 100 kHz, and a four channel, chopped-beam, Tektronix type 1A4 amplifier. A Tektronix oscilloscope camera was used to record the data.

Pressure in the chamber was measured with an MKS baratron pressure meter, type 144. The flow of argon gas into the chamber was measured with flow meters calibrated in standard cm^3 per sec for argon.

To analyze the data from the probes a computerized system was used. The basic components were a Hewlett Packard 2116C computer, an HP digital voltage source (DVS), and an HP digital voltmeter (DVM), types 6130B and 2116C. The DVS and DVM were both controlled directly by the computer. The DVS was used to impress voltage on a selected probe and the amplified current was then measured and fed directly into the computer. The program used is listed in Appendix A, with a brief discussion of the main features of the program.

III. Experimental Procedures and Results

General Approach

The first step in studying plasma instabilities in the ELMAX was obviously to find some instabilities, that is, to determine what values of the various control parameters available would result in an instability being observed. An integral part of this step was deciding how to observe the instability if it did occur. After the first step had been accomplished, the next step was to determine what characteristics of the instability could be observed, and what plasma parameters could be measured, which would allow the instability to be compared to known types of instabilities and thus to identify it.

Control Parameters - Finding the Instabilities

There were four control parameters which were systematically varied during the search for instabilities. These were: magnet current, gas flow rate, current to the magnetrons, and current to the spiral cathodes. In addition to these control parameters, the polarity of the voltage across the spirals could be reversed, the spiral grounding could be changed, and the magnet current could be reversed. Variation of these control parameters cannot be directly related to the resulting variation in plasma parameters because of the very complicated interrelations which are present. For example, variation of the magnet current not only changed the magnetic

field but also changed the density and temperature profiles of the plasma. In the same way, variation of the current of the spirals was found to affect not only the observed values of temperature and density, but also the frequency and radial position of the observed oscillations. For this reason the control parameters and plasma parameters were treated as distinct from one another. Control parameters were varied to change the plasma being studied and then plasma parameters measured as if they were independent variables. To detect any instabilities which might occur, the floating potential from at least two probes, usually the two probes at the center of the chamber, was displayed on the oscilloscope. The oscilloscope was monitored at all times when control parameters were being varied. If an oscillation appeared which might indicate the presence of an instability, pictures of the scope trace and of the spectrum analyzer display were made, and all control parameters were recorded. At first, no useful results were obtained using this technique. Many alternate methods of detecting instabilities were considered but no acceptable alternative was found. Fortunately, during this time, the ELMAX system was being gradually improved. Analysis of data from previous experiments showed that higher magnetic fields than those being used in the present experiment had resulted in a relatively quiet plasma with what appeared to be discrete oscillations sometimes present. This indicated that increasing the current available to the magnets might improve results. The current available was increased by about twenty percent.

It was also noted that the power supplies to both the magnetrons and the spiral had significant amounts of ripple in their output voltage which might have been obscuring the results of an instability. Filters were installed which significantly reduced these ripples. With these improvements, useful oscillations began to be detected.

Plasma Parameters-Recording Instability Characteristics

Having detected useful oscillations the next step was to record as many plasma parameters as possible while the instability was present, and to observe and record whatever other characteristics could be detected. The computer analysis of the probe curve provided the means of measuring the plasma parameters. The parameters which were available from the computer analysis included: electron temperature, ion density, floating and space potential, and Debye length. By varying the probe position by a small amount, usually one-quarter or one-half cm, and repeating the computer analysis, all of these parameters were available as functions of radial probe position. This in turn allows the calculation of the gradients of these parameters. A typical computer output sheet is shown in Appendix A.

The frequency of the oscillation was measured with the spectrum analyzer, and phase relations between the floating potential oscillations at the various probe positions were recorded, using pictures of the scope trace. By biasing the

probe with the proper voltage, it was driven into the ion-saturation portion of the probe curve. Oscillations in the current drawn by the probe are therefore primarily related to ion density fluctuations and allow a measurement of the phase relation between density and potential at that probe. This phase relation is an important characteristic of the oscillation since different types of instabilities will cause different phase relations between density and potential. For example, drift wave instabilities usually have the density wave leading the potential wave, while flute instabilities normally result in oscillations with the opposite density-potential phase relation.

The potential measured in this experiment is the floating potential of the probe. Since the density-potential relationships discussed above are actually derived theoretically using the space potential of the plasma, it would be very helpful to determine the exact phase difference, if any, between the space and floating potential. This phase difference is often assumed to be negligible, and in the paper used to compare experimental results from this study with theoretical predictions no distinction is made between space and floating potential. However, an experiment was devised which would measure the phase relation between density and floating potential and between density and space potential to insure the validity of the assumption that no significant phase difference existed between the two potentials. To accomplish these measurements, a "Boxcar" integrator was used. Although this

device is rather complicated, the principles of operation are straightforward. The boxcar accepts two inputs, the first input being the varying amplitude of a given wave, and the second being a trigger pulse synchronized in some way with the input wave. The "Boxcar" then samples the wave amplitude during some small time interval at a phase point of the incoming wave determined by the trigger pulse. Adjusting the trigger pulse to coincide with consecutive phase points along the incoming wave allows the characteristics of the wave to be determined as a function of phase position. In this experiment, the input wave was the output of the Langmuir probe as the biasing potential was varied to generate the probe curve. The output of the "Boxcar" was then used as the input to the computer which analyzed the probe curve. In this way the various plasma parameters, specifically the temperature, density, and potential were calculated as a function of phase position of the oscillation. By plotting these variables versus the phase position, the relation between these variables could be determined. The results of this experiment were inconclusive for two reasons. First, several hours were required to complete one run through one wavelength of the oscillation. When the beginning of the run was repeated immediately after completing a run, to check the repeatability of the results, different results were obtained. Second, a careful analysis of the output of the "Boxcar" revealed that the output was not maintaining a constant relation to the input amplitude as it should have.

The results of this particular experiment were therefore not used.

Experimental Results

Continuous, almost sinusoidal oscillations were observed over a wide range of control parameters. These oscillations had an apparent clockwise phase velocity as looking along the magnetic field and in the direction of the magnetic field. To facilitate discussion, the direction of the magnetic field, which was parallel to the longitudinal axis of the vacuum chamber, is designated as the positive z-direction. Then the r and theta directions are designated as the other two directions, the apparent phase velocity of the oscillations as in the positive theta direction. Wave-length along the z-axis could not be measured exactly, since probes could be inserted at only three points along the z-axis. If the three probes along the z-axis were all adjusted to the same radial position, the center probe showed the largest amplitude; however, if the three probes were adjusted to the radial distance which gave the largest amplitude for that probe, the three amplitudes were approximately the same. For the oscillations which are analyzed in detail in this study, the center probe had the largest oscillation at a radial position of 3 cm. The two end probes showed the maximum oscillations when positioned at 2.5 cm. When the probes were adjusted to these positions, no phase difference between the three probes could be detected. These observations can be explained if a longitudinal standing wave is assumed to exist in the plasma. The boundary conditions for

this standing wave would be the physical characteristics of the chamber. Since the first conducting surface which was in contact with the plasma at each end of the chamber was the spiral cathode, the wavelength of the standing wave must be some integral multiple of the distance between the two spirals. A wavelength equal to this length would result in a minimum amplitude at the center of the chamber. Since this was not observed, the wavelength of the standing wave must equal at least twice the distance between the spirals.

To determine the wavelength of the oscillations in the theta direction, the output of two probes in the same r-theta plane were compared on the oscilloscope, using a copped sweep on the oscilloscope so that the phase relation between the two signals could be seen. When using the center probes, which were positioned 90 degrees apart, a phase relation of either 90 or 180 degrees was observed. The change from one phase relation to the other was always accompanied by an apparent doubling of frequency and was caused by a change in the applied magnetic field. This was interpreted as a mode change. The term "mode" as used here refers to the ratio between the circumference of the plasma column at the radial position at which the oscillation is detected and the wavelength of the oscillation. Since the oscillation is observed to be continuous, the wavelength must be equal to the circumference divided by some integral number. If this were not true, interference would occur at some point around the plasma column and a continuous oscillation

would not be observed. If $\lambda_\perp$ is the wavelength of the oscillation in the theta direction, and $K_\perp$ is the wave number, then

$$K_\perp = 2\pi(\lambda_\perp)^{-1} = 2\pi(2\pi P/M)^{-1} \quad (1)$$

$$K_\perp = 2\pi M/2\pi r = M/r \quad (2)$$

where M is the mode number. When an apparent phase shift of 90 degrees is observed between two probes positioned 90 degrees apart, this is interpreted to mean that the same maximum potential arrives at the second probe one-fourth of a cycle after it reached the first probe. This is called an m=1 mode. If the phase shift appears to be 180 degrees, this means that one probe is sensing a minimum potential while the other is sensing a maximum. This is interpreted to mean that the wavelength of the oscillation is equal to one-half of the circumference, that is, m=2.

The sketches in Fig. 2 illustrate the results of a sequence of spectrum analyses of the oscillation. The input to the spectrum analyzer was the floating potential from a probe at the center of the chamber, radially positioned to the point of maximum amplitude of the oscillation. The magnetic field was increased after each analysis was made so the sequence illustrates the behavior of the oscillation as a function of magnetic field. Fig. 2(a) shows a mode 1 oscillation with a frequency of 8 kHz. With the magnetic field increased, Fig 2(b) shows a decrease in the frequency of the mode 1 oscillation to 6 kHz and at 12 kHz can be seen the beginning of a mode 2

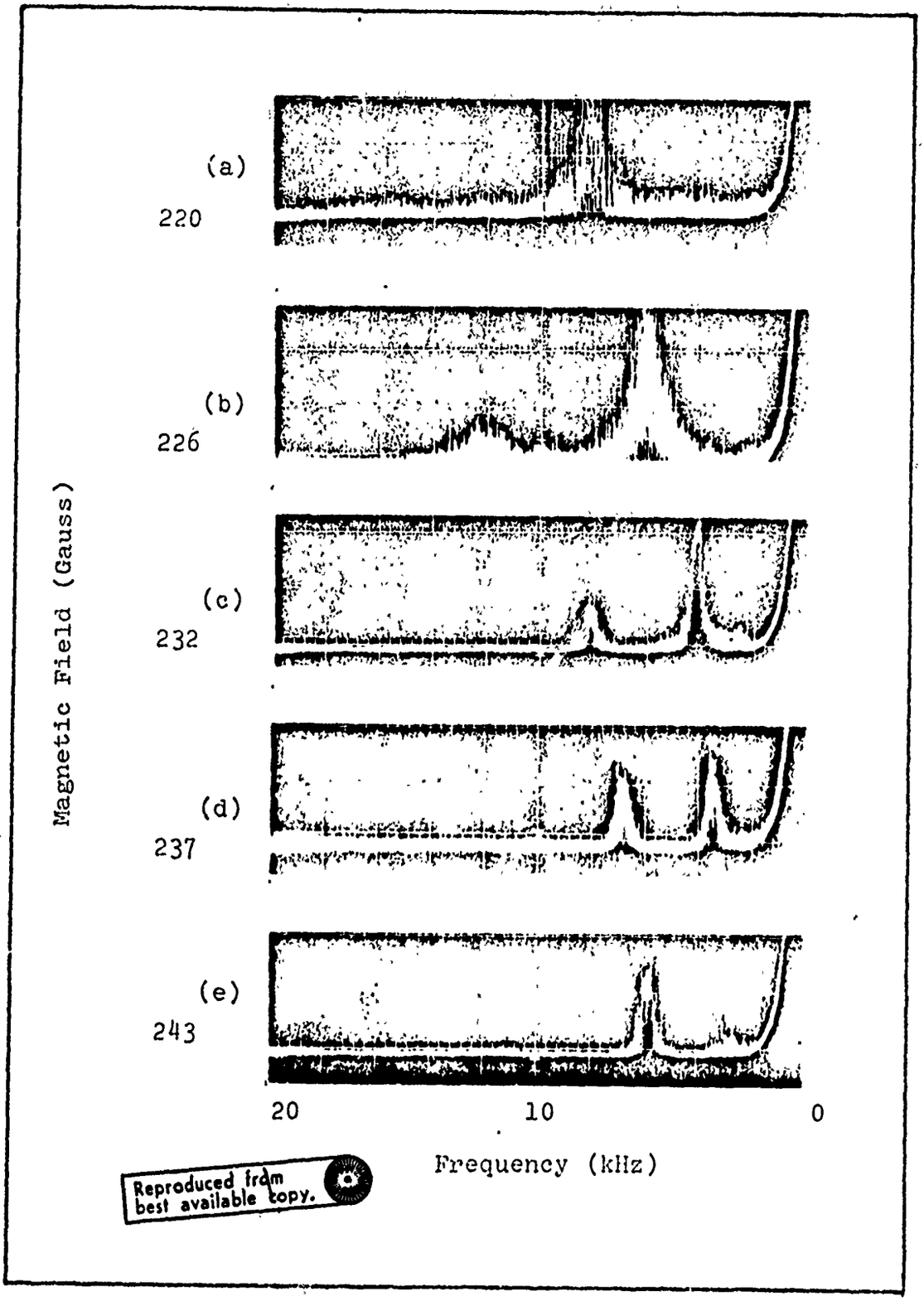

Fig. 2 Spectrum Analyses of Oscillations

oscillation. Fig. 2(c) shows the continuing decrease in frequency of both modes as the magnetic field is increased. The increase in the amplitude of the mode 2 oscillation and the decrease in the amplitude of the mode 1 can clearly be seen in Fig. 2(d) and 2(e). In Fig. 2(e) the mode 1 oscillation has almost completely disappeared, while the mode 2 oscillation has reached its maximum amplitude and continued to decrease in frequency.

To determine the phase relation between the density and potential oscillations, a probe was biased with a negative voltage so that the current drawn by the probe was a measure of the ion density in the plasma surrounding the probe. The current was then amplified and displayed on the oscilloscope to determine the phase relation between density and potential. The density was found to lead the potential by approximately 90 degrees, both in mode 1 and mode 2.

The oscillations were observed over a wide range of control parameters. The limits were usually imposed by equipment limitations rather than the loss of the oscillations. The magnetic field ranged from 200 gauss to 250 gauss in the center of the chamber. No oscillations were observed below 200 gauss and 250 gauss required the maximum magnet current available. Oscillations were found only in the upper twenty percent of the range available in spiral current. This range corresponds to the largest density gradients which were found in plasma density. Pressure could be varied from about 0.4 microns of H_g to about 2.5 microns without losing the oscillations, but were primarily studied at a pressure between 1.5 to 2.0 microns because

the conditions were the easiest to maintain in this pressure region. Control of the power to the magnetrons, and adjustment of the stub tuners was not used primarily to vary the plasma parameters, but rather were both adjusted so as to insure equal production of plasma at both ends of the chamber with a minimum amount of noise in the magnetron circuits. This was done to minimize the presence of source-generated oscillations in the plasma.

Reversing the current to the magnets resulted in no apparent change in the oscillations, other than a reversal of the theta phase velocity relative to the chamber, as expected.

Reversing the polarity of the spiral voltage resulted in a hollow plasma with maximum density occuring at about 3 cm rather than at the center of the plasma. This plasma configuration was not studied because of the large amount of noise present in the probe outputs and because of the undesirable density profile.

With this knowlege of the general characteristics of the oscillations, a general, qualitative comparison of the instability responsible for the oscillations could now be made. For a quantitative comparison, however, some information on the variation of the plasma parameters was required. To obtain this information, radial scans of the plasma electron temperature, the ion density, and the space potential of the plasma were made. This was done by making a computer run with the probe in a given radial position and obtaining a computer output which gave the desired parameters at that probe position. The probe was then moved to a position a small distance from the first position and another computer run was made. The plots shown in

Fig. 3 through Fig. 8 display the ion density and electron temperature as a function of probe position. Fig. 3 shows the parameters as measured at the top probe with a mode 1 oscillation present in the plasma. Fig. 4 gives the parameters with the magnetic field reduced until the oscillations disappear. Fig. 5 gives the same information as Fig. 4 except that the oscillations were removed by reducing spiral current rather than magnetic field. Fig. 6 through Fig. 8 give the same information, except that the end probe was used rather than the center probe.

The significance of the data given in Fig. 3, 4, and 5 can best be seen by comparing the data observed with the oscillations present to each of the two cases with the oscillations not present. The temperature variation is very slight in either case, however the density with oscillations present (Fig. 3) is three times as great as with no oscillations due to reduced magnetic field (Fig. 4) but only half again as large as the density when the oscillations are removed by reducing the current to the spiral cathodes. As is discussed in comparing the observed oscillations with known types of oscillations, the density gradient emerges as the important factor rather than the density itself. The same relations are seen in Fig. 6, 7, and 8 for the data taken from the end probes.

Although space potential is calculated in the program used, it is not plotted because it was found not to be useful in determining the nature of the instability causing the observed

oscillations. Near the end of this study, some improvements in the computer program was made which caused different values to be calculated for space potential. This occurred too late for new runs to be made, however, so no valid information about the space potential is available for this study.

Another plasma parameter which would aid in a quantitative comparison of the observed instabilities with known theory is the ion temperature. No method was available during this study to measure ion temperature.

The frequency observed ranged from 3 kHz to 8 kHz and exhibited a strong dependence on magnetic field. As the magnetic field is increased, the observed frequency decreases until a mode change occurs. At this point, the frequency doubles and then begins to decrease again with increasing magnetic field.

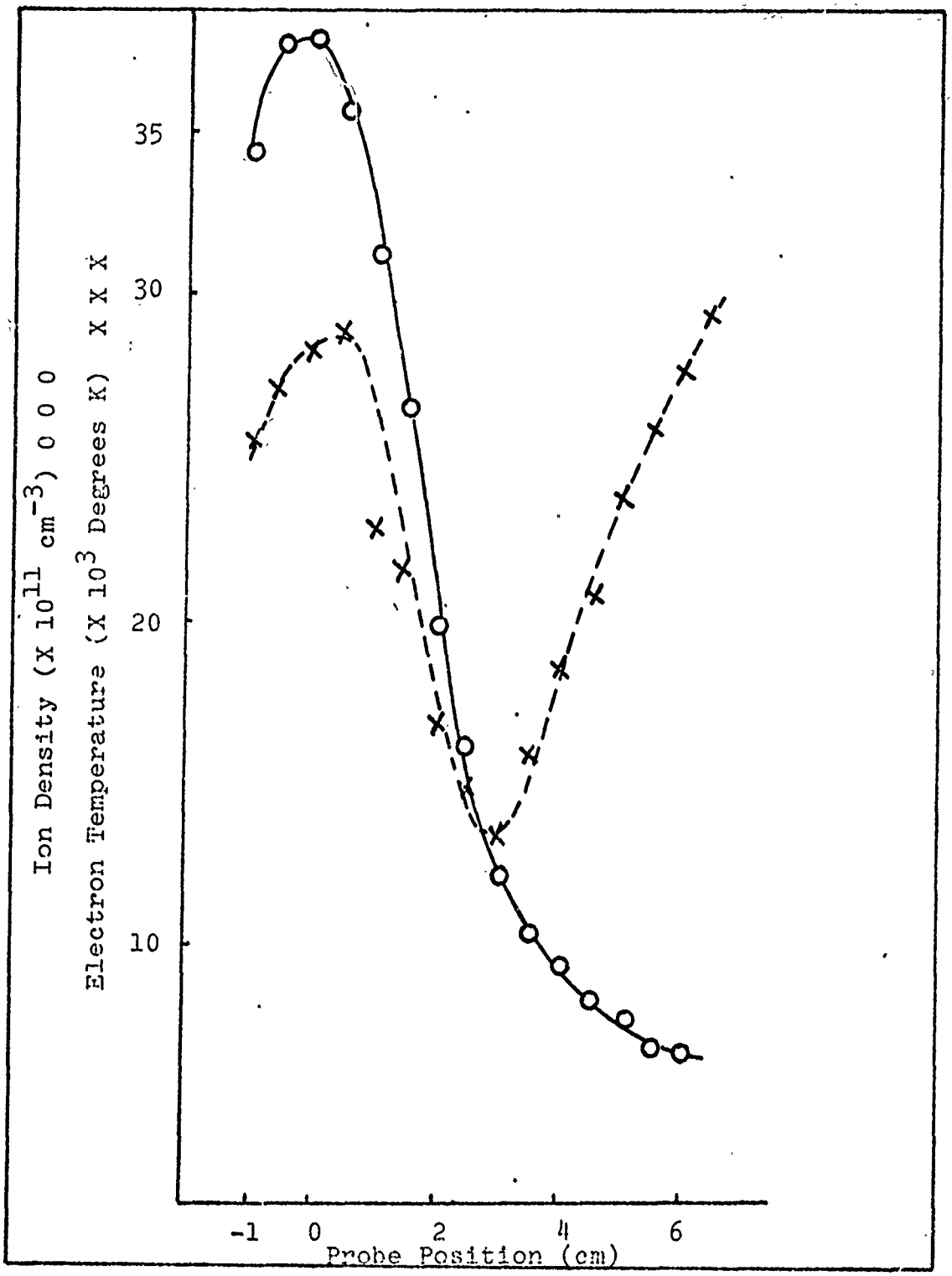

Fig. 3 Center Probe with Mode 1 Oscillations

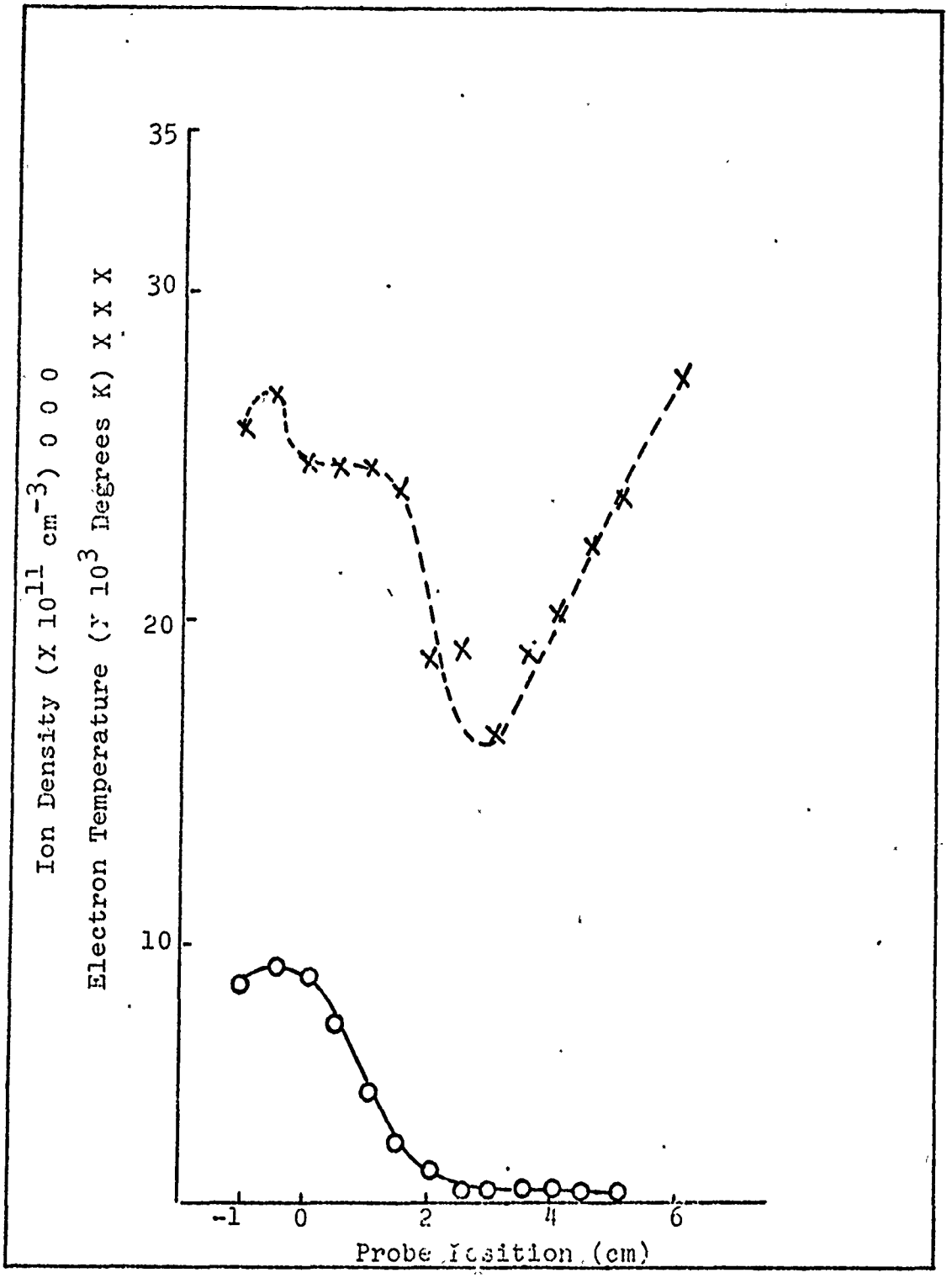

Fig. 4 Center Probe - Reduced Magnetic Field

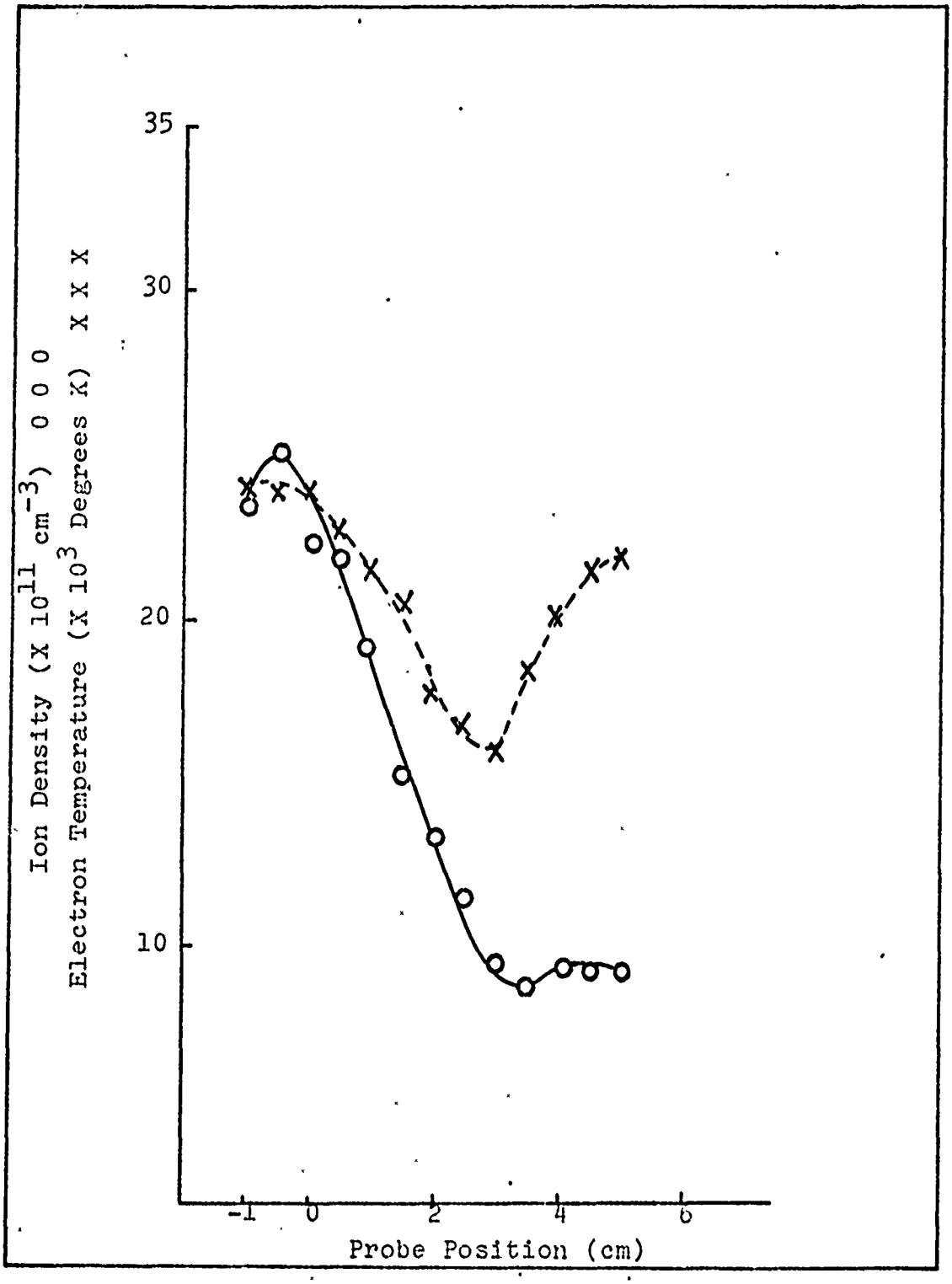

Fig. 5 Center Probe - Reduced Spiral Current

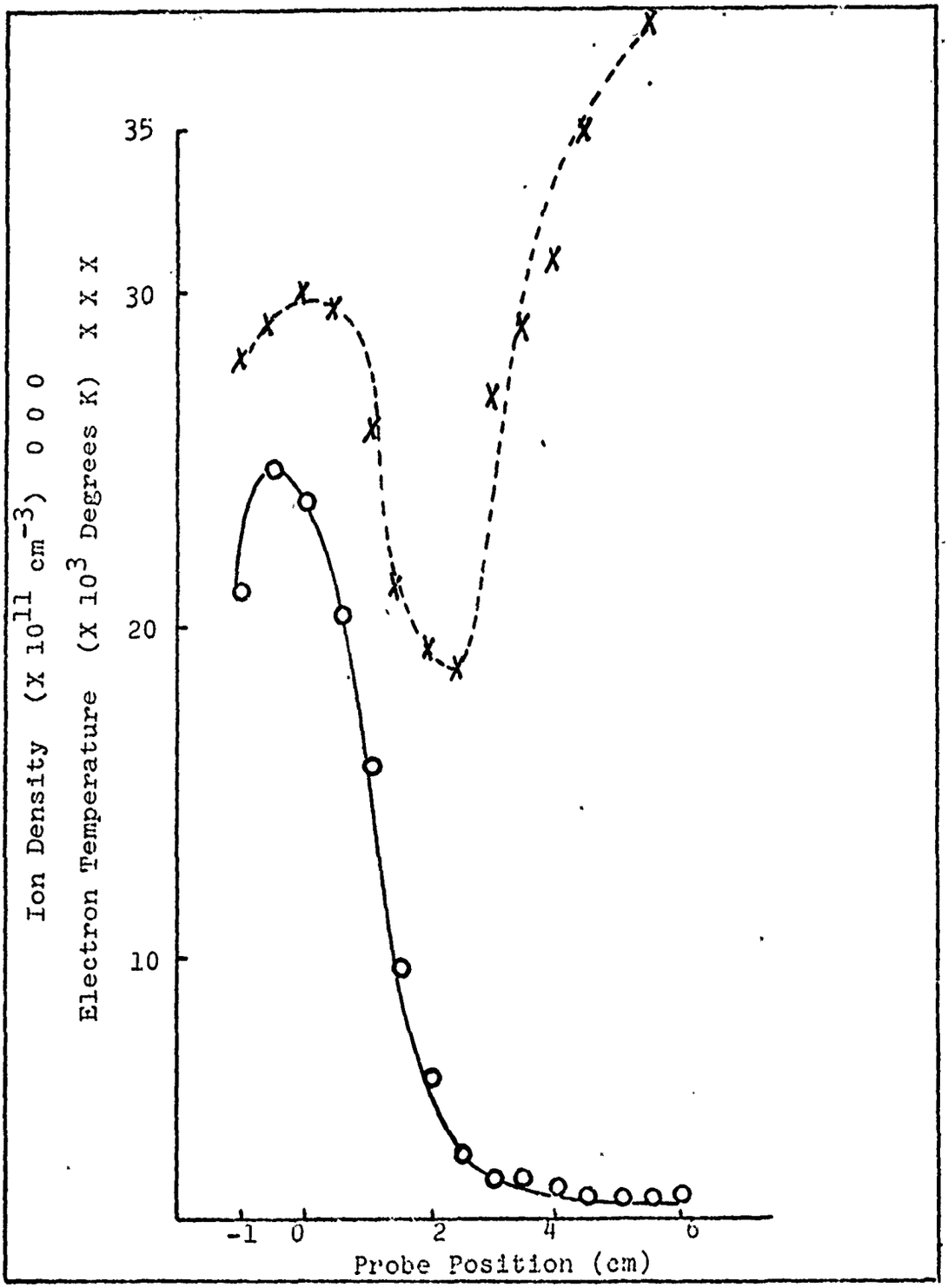

Fig. 6 End Probe With Mode 1 Oscillations

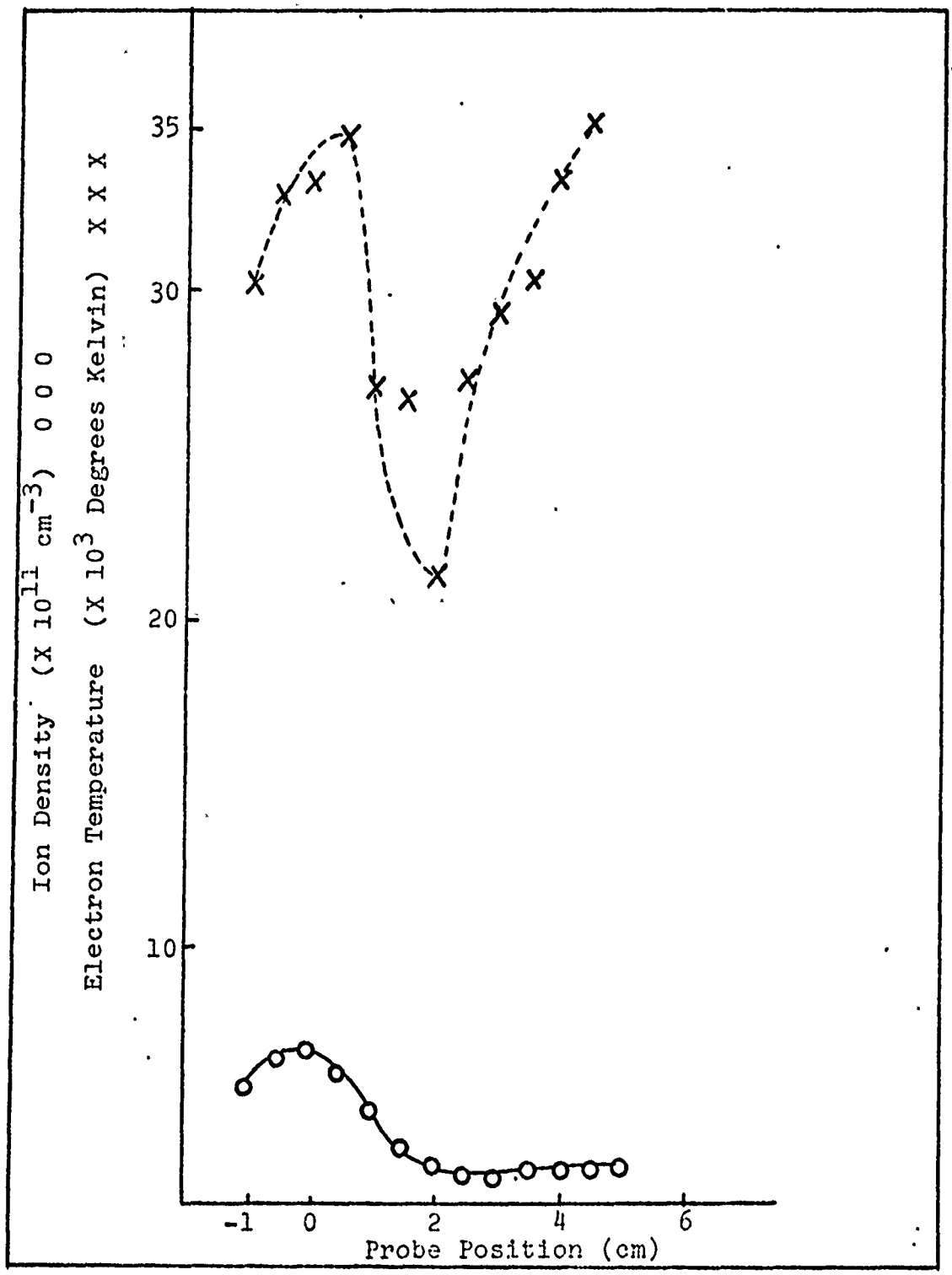

Fig. 7 End Probe - Reduced Magnetic Field

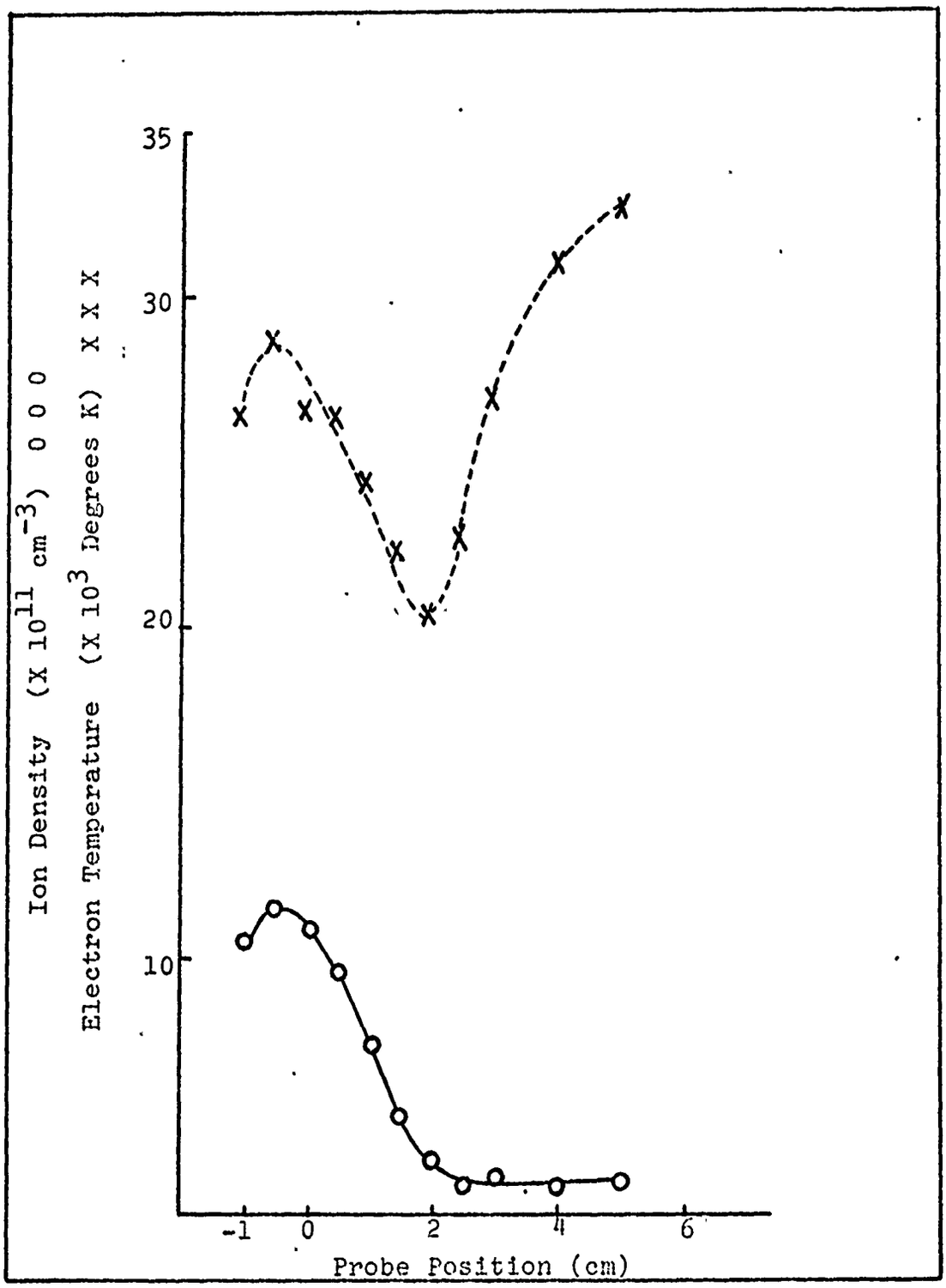

Fig. 8 End Probe - Reduced Spiral Current

IV. Theory

The very large number of known instabilities makes a comparison of a given experimentally observed instability with all known instabilities almost impossible. The literature survey by Auer, et al. proved invaluable in making the comparison. This survey lists 136 known instabilities and cites references for each. Many of the instabilities listed could be eliminated immediately because of some obvious disagreement with the observed characteristics. For example, all of the ion-cyclotron instabilities were eliminated just on the basis of the frequency observed being much too low for this type of instability. (Ref 2)

Many other instabilities would exhibit experimental characteristics which are in agreement with those observed, but can be eliminated on the basis of some one calculated plasma parameter, such as one of the collision frequencies. An example of this type is the Simon-Hoh instability (Ref 3:383) which was eliminated because the ion-neutral collision frequency is too low in the experimental plasma (Ref 4:14).

The Kelvin-Helmholtz instability was considered to be almost identical to the observed instability until the parallel wavelength was measured. Since the Kelvin-Helmholtz wave is characterized by short parallel wavelengths, the observation of long parallel wavelengths allowed elimination of this instability (Ref 5:818).

Temperature-gradient-driven drift instabilities also exhibit characteristics very similar to the observed waves, however, they are stabilized by the presence of a density gradient and one stability criterion is a simple relation between the density and temperature gradients which the experimental plasma does not satisfy (Ref 6:1107).

There were two types of instabilities which were considered which could not be eliminated. These were the collisional drift instability and the flute instability. The term "collisional" as used here refers only to the mechanism which restricts the motion of electrons parallel to the applied magnetic field. As a convenient measure, the drift instability is considered collisional if the mean free path of the electrons between collisions with ions is less than the parallel wavelength of the oscillation. Flute instabilities are almost always considered probable in a mirror-type geometry unless some provision such as Ioffe bars are employed to suppress them. Drift instabilities have been found in almost all kinds of confinement schemes, and are in fact so common that they are often called "Universal Instabilities." The two instabilities are very similar to each other, and in fact the flute is often treated as a special case of the drift instabilities. (Ref 7:154-156)

Quantitative Comparison With Flute Instability

The dispersion relation for the flute instability as given by Schmidt (Ref 7:283-294) is used in this analysis. This dispersion relation leads to the stability condition

$$K^2/\Omega^2 \ (g + u_T^2 n^1/2n_0)^2 \geq 4g \ n^1/n_0 \qquad (3)$$

where K is the perpendicular wave number, Ω is the ion cyclotron frequency, g is the effective gravity, u_T is the thermal speed of the ions and n^1/n_0 is the normalized density gradient. If the plasma is assumed to be nearly thermal, and no radial electric field is considered, then $g = (\frac{3}{2}) \ U_T^2/R$. If the inequality in Egn. 3 is not satisfied, unstable oscillations result. Using data from the top center probe where flute instabilities are most likely to occur and assuming ion temperature to be about 300 degrees Kelvin, the values for the experimental plasma are

$$K = 1 \times 10^3 \ m^{-1}$$
$$\Omega = 5.5 \times 10^4 \ \text{rad sec}^{-1}$$
$$U_T^2 = 6.2 \times 10^4 \ m^2 \ \text{sec}^{-2}$$
$$g = 1.9 \times 10^4 \ m \ \text{sec}^{-2}$$
$$n^1/n_0 = 49 \ m^{-1}$$

and the inequality is not satisfied. However, solving the dispersion relation for the real part of the frequency gives a value of less than one kHz which does not agree with the observed frequency. In addition, since the drift velocity imparted to the electrons and ions by a flute instability is proportional to the mass of the particles, the drift of the electrons is negligible compared to the ion drift velocity and therefore, the oscillation travels in the direction of the ion

drift velocity. This results in the potential wave leading the density wave which is the reverse of the observed relation. Both of these difficulties can be overcome if a radial electric field is assumed such that the plasma column rotation would give an apparent observed frequency of 4 kHz. With such an electric field, the doppler shift due to the plasma E×B drift would dominate the oscillation's phase velocity and the density-potential phase relation would be reversed. In such a case however, the value of g would be changed by the addition of a term V^2/R where V is the tangential velocity of the plasma and R is the distance from the center of rotation. To give the proper frequency, $V^2/R = 9.6\times10^{5m}$ sec^{-2} and g becomes 9.78×10^{5m} sec^{-2}. When this new value for g is inserted into Eqn. 3, the inequality is satisfied and no instability will occur. Justification for the added term for the effective gravity is given by Bhatia (Ref 9:1652). The resulting stability is predicted by Vlasov (Ref 10:486).

Quantitative Comparison With Drift Instability

During the literature search for this study, a paper written by Hendel and Politzer (Ref 11) was found which appeared to give almost identical results to the ones obtained during this study. Subsequently, a later paper by Hendel, Chu and Politzer was found which derived a dispersion relation explaining the results of the earlier paper. The observed characteristics of wave number (both parallel and perpendicular), frequency range, density-potential phase

relation, and the dependence of frequency and mode number on magnetic field were all in agreement with the observations made by Hendel, et. al. (Ref 12).

The dispersion relation used by Hendel, et al. is derived using linear theory and a slab model for the plasma. In the regime of parameters found in the experimental plasma in this study, the resulting stability condition reduces to

$$K_{11}^2 \, (n^1/n_0)^{-2} > (m_e/m_i)^{\frac{1}{2}} \tag{4}$$

where K_{11} is the parallel wave number, n^1/n_0 is the normalized density gradient, m_e is the electron mass and m_i is the mass of the ions. Using data from the end probes, this stability condition not only predicts instability when the oscillations are observed, but also predicts stability when the oscillations are eliminated by reducing either spiral current or magnetic field. The correct predictions are considered the best indication that the observed oscillations are indeed caused by a collisional drift instability.

For a numerical analysis, Eq(4) can be rearranged to read

$$K_{11}^2 \, (m_e/m_i)^{-\frac{1}{2}} > (n^1/n_0)^2 \tag{5}$$

For argon atoms, $(m_e/m_i)^{\frac{1}{2}}$ equals 3.69×10^{-3}. If λ_{11} is equal to twice the distance between the spiral cathodes, K_{11}^2 equals 6.85×10^{-4} cm^{-2}, and the stability condition becomes

$$0.185 \text{ cm}^{-2} > (n^1/n_0)^2 \text{ cm}^{-2} \tag{6}$$

or the equivalent statement, the wave grows if

$$|n^1/n_0| > 0.430 \text{ cm}^{-1} \tag{7}$$

Since the maximum amplitude oscillations were observed at a radial position of 3.0 cm for the center probes and 2.5 cm for the end probes, $|n^1/n_0|$ is calculated at these positions from the data given in Figs. 3 through 8. For the center probes $|n^1/n_0|$ equals:

0.49 - with oscillations

0.12 - with reduced magnetic field and no oscillations

0.28 - with reduced spiral current and no oscillations

For the end probes $|n^1/n_0|$ equals:

0.80 - with oscillations

0.23 - with reduced magnetic field and no oscillations

0.20 - with reduced spiral current and no oscillations

The theory agrees with observation in all cases and oscillations are observed only when the inequality in Eqn. (7) is satisfied.

V. Conclusions and Recommendations

The purpose of this study was to find experimentally and to identify, using existing theory, the dominant instabilities in the ELMAX plasma device. The good agreement between the theory developed by Hendel, et. al. was very satisfying. The recommendations which are suggested by the results obtained are simple and obvious. The need to be able to measure ion temperature and parallel wave-length were in fact already known and under consideration before the study began. The study did point out the need for a better way to measure the space potential so that the electric field in the plasma could be calculated.

The follow-on experiment is already under way and some initial success with suppression of the observed oscillations lend some support to the conclusions reached. In particular, suppression of the oscillations using suppressor probes located near the end of the chamber, where the observed density gradient is the largest and where, therefore, the oscillations are predicted to be most likely to grow, lends support to the conclusions reached.

The real conclusion of this study must wait until the experiments on feedback stabilization have been completed.

Bibliography

1. Nunn, J. R. "Langmuir Probe Diagnostics in the ELMAX Plasma Device." M. S. Thesis, Air Force Institute of Technology, Ohio, 1971.

2. Auer, G., et al. "Literature Survey on Plasma Instabilities." Scientific Report N R 75. Institute for Theoretical Physics. Austria (Europe) (December, 1972).

3. Simon, A. "Instability of a Partially Ionized Plasma in Crossed Electric and Magnetic Fields." Physics of Fluids, 6 : 382-388, (1963).

4. Brown, S. C. Basic Data of Plasma Physics (Second Edition) Massachusetts: The M.I.T. Press, 1967.

5. von Gaeler, S. "Relation Between the Kelvin-Helmholtz Instabilities." Physics of Fluids 9 :818-820, (1966).

6. Jukes, J. D. "Effect of Temperature Gradient on Plasma Stability." Physics of Fluids, 10 : 1107, (1967).

7. Krall, N. A. "Drift Waves" in Advances in Plasma Physics, edited by Simon and Thompson, New York : Interscience Publishers, 1968.

8. Schmidt, G. Physics of High Temperature Plasmas. New York : Academic Press, 1966.

9. Bhatia, P. K. "Gravitational Instability of a Rotating Anistropic Plasma." Physics of Fluids, 10 : 1652, (1967).

10. Vlasov, M. A. and Krivtsov, V. A. "Influence of a Radial Electric Field on the Instability of an Inhomogeneous Plasma." Soviet Physics JETP 24, No. 3:486-491, (1967).

11. Hendel, H. W. and Politzer, P. A. "Collisional Drift Instability in Non-Isothermal Plasmas." Proceedings of Conference on Physics of Quiescent Plasmas. Frascati, Italy: Associazione Euratom, 1967.

12. Hendel, H. W. et al. "Collisional Drift Waves- Identification, Stabilization and Enhanced Plasma Transport." Physics of Fluids, 11 : 2426-2439, (1968).

13. Laframboise, James G. "Theory of Spherical and Cylindrical Langmuir Probes in a Collisionless, Maxwellian Plasma at Rest." UTIAS Report No. 100 (1966).

Appendix A

Computer Program Used In Analysis

The computer program used in the calculation of electron temperature and ion density is listed in FORTRAN in this appendix, immediately following fig. 9. Fig. 9 shows a typical computer output from the program. The program is designed to analyze the characteristics of a probe curve, which is the plot of probe current versus probe voltage. The program is written to use a variable number of points in the analysis but normally 250 points were used. In Fig. 9 the first numerical entry is simply entering the number of points to be used. To generate the probe curve, a minimum and maximum voltage are selected by trial and error to include both ion saturation current and electron saturation current. In the run which resulted in Fig. 9, these values are -23 volts and +1 volt. The next entries tell the computer which probe is being used and the radial position of the probe. The last entry refers to the gain on an amplifier used in the probe current circuit.

Since the probe current is the sum of the electron and ion current, a straight line approximation of the ion current is made, and then subtracted from the total current to give electron current. The approximation used is the next item given in Fig. 9. Next follows a listing of selected currents and probe voltages with the "INDEX" showing at which of the 250

points they occured. This read-out helps in the initial selection of the maximum and minimum voltages used and is also helpful in analyzing the operation of the computer.

To calculate the electron temperature, a non-dimensional potential is defined and the electron current equation is written as an exponential function of this potential. Since the defined potential is a function of electron temperature, a plot of the natural log of electron current versus potential yields a straight line, the slope of which determines the electron temperature.

Since the current at ion saturation is a function of the ion density, a value for density can be calculated once the ion current is known. In this program the density is calculated several ways and four different densities are shown on the computer output. In this study the one selected is calculated using theory developed by Laframboise assuming ion temperature to be zero (Ref 13). The selection of this particular density is not too important since in this study the absolute value of the density is not important, but rather the density gradient. All of the densities given by the program yield approximately the same gradients. The electron temperature is shown in Fig. 9 as "TE at (IFL)" and is given in degrees Kelvin. The density appears as the last entry under "DENSITY."

```
ENTER RUN NUMBER
1

ENTER; NUMBER OF POINTS
       VMIN,VMAX
       PROBE NUMBER,POSITION (CM)
       CONVERTER GAIN
250
-23,1
2,-1
.1


ION CURRENT APPROXIMATION ( 51.9 INCREMENTS)
  CI = .1593E+01 * V + -.4557E+02     EMAX = .8600E+01
  ZERO ION CURRENT AT 28.60 VOLTS

      INDEX        V            CP           CES
MIN       1    -.1533E+02   -.6445E+02
MI      106    -.5205E+01   -.5675E+02
MM1     113    -.4530E+01   -.5120E+02    .3101E+01
MM3     120    -.3655E+01   -.4980E+02    .3196E+01
IFL     160     .0000E+00    .1200E+01    .6176E+02
ISP     203     .4145E+01    .2260E+04    .2446E+04
MM4     236     .7325E+01    .5225E+04    .4669E+04
MM2     243     .8000E+01    .5321E+04    .4858E+04
MAX     250     .8675E+01    .5594E+04

TE AT V(IFL) = 12515. DEG K     EMAX = .4339E-01

SHEATH CALCULATIONS
     14.07 VOLTS BELOW V(ISP) (146.0 INCREMENTS)
     BETA2 = .1978E+01
     SHEATH THICKNESS = .7032E-04
     RADIUS = .1145E-03 METERS
     LENGTH = .9786E-03 METERS
     RP/RS = .3859E+00

ION NUMBER DENSITY =
      .12419E+13 AT V(IFL)
      .50325E+12 AT V(IFL)-10 (USING SHEATH)

   DEB     TI/TE     RP/LD      VPF      DENSITY
.869E-03     1     .512E+01     4.98    .789E+12
.773E-03     0     .574E+01     5.24    .999E+12
PAUSE
PAUSE
```

Fig. 9 Typical Computer Output

Appendix A

```
0001  FTN,B
0002        PROGRAM DATA9
0003        COMMON V(250),CMS(250),CE(250),A(8),B(8),C(8),ALCES(250)
0004       *TS(250),SDCES(250),D(2),TR(2),TXL(2)
0005        CALL CLPS
0006        NUL=8
0007        E=1.6021E-19
0008        XK=1.3805E-23
0009        TEN6=1.E-06
0010        A(1)=0.15113
0011        A(2)=0.14661
0012        A(3)=0.13303
0013        A(4)=0.11041
0014        A(5)=0.078733
0015        A(6)=0.038009
0016        A(7)=-0.011765
0017        A(8)=-0.070588
0018        B(1)=0.0
0019        B(2)=3.5714E-3
0020        B(3)=7.1429E-3
0021        B(4)=1.0714E-2
0022        B(5)=1.4286E-2
0023        B(6)=1.7857E-2
0024        B(7)=2.1429E-2
0025        B(8)=2.625
0026        C(1)=-9.0493E-3
0027        C(2)=-8.5650E-3
0028        C(3)=-7.1105E-3
0029        C(4)=-4.6865E-3
0030        C(5)=-1.2928E-3
0031        C(6)=3.0705E-3
0032        C(7)=8.4034E-3
0033        C(8)=1.4706E-2
0034        XM=40.
0035        XMP=1.6725E-27
0036        XME=9.1091E-31
0037        PI=3.14159
0038        EPS=8.8553E-12
0039        WRITE(2,1000)
0040  1000  FORMAT (7/"ENTER; DATE"/7X,"DIAMETER AND LENGTH (IN IN
0041       *CHES) OF PROBE 1"/7X,"DIAMETER AND LENGTH OF PROBE 2"/
0042       *7X,"VIS,VFP,VSP")
0043        READ(1,1030)NUM1A,NUM1B
0044  1030  FORMAT(2I3)
0045        DO 180 I=1,2
0046        READ (1,*) TR(I),TXL(I)
0047        TR(I)=TR(I)*2.54E-2/2.
0048  180   TXL(I)=TXL(I)*2.54E-2
0049        READ(1,*)VIS,VFP,VSP
0050        CALL LEADR(8,20)
0051  10    PAUSE 1
0052        WRITE(2,1010)
0053  1010  FORMAT (5/"ENTER RUN NUMBER")
0054        READ(1,*)NUM2
0055  40    WRITE (2,1020)
0056  1020  FORMAT (/"ENTER; NUMBER OF POINTS"/7X,"VMIN,VMAX"/7X,
0057       *"PROBE NUMBER,POSITION (CM)"/7X,"CONVERTER GAIN")
0058        READ (1,*) NE
0059        READ (1,*) V(1),V(NE)
```

```
0060          READ (1,*) IP,CM
0061          READ (1,*) GAIN
0062          R=TR(IP)
0063          XL=TXL(IP)
0064          DV=(V(NW)-V(1))/FLOAT(NW-1)
0065          DO 20 I=2,NW
0066    20    V(I)=V(I-1)+DV
0067          VS=V(NW)-V(1)
0068          CALL SWR (14,ID)
0069          IF (ID) 31,32
0070    31    WRITE (2,7100)
0071    7100  FORMAT (//"ANALYTIC GENERATION"/"ENTER X1,X2 FOR RANGE
0072         *OF X")
0073          READ(1,*)X1,X2
0074          DX=(X2-X1)/FLOAT(NW)
0075          X=X1
0076          DO 710 I=1,NW
0077          CPEL=5000.*(1.+TANH(X))
0078          CPION=5.*X-10.
0079          CPHIE=20.*(1.+TANH(3.*(X+2.)))
0080          CE(I)=CPEL+CPION+CPHIE
0081    710   X=X+DX
0082          DO 25 I=1,NW
0083    25    CE(I)=CE(I)/GAIN
0084          GO TO 5
0085    32    CONTINUE
0086          DO 33 I=1,NW
0087    33    CE(I)=0.
0088          GAIN=10.*GAIN
0089          NCODE=4
0090          WRITE (10) NCODE
0091          DO 30 I=1,NW
0092          CALL DVS (V(I))
0093          DO 35 J=1,10
0094          READ (10,1040) IS,TCE
0095    1040  FORMAT (1X,I1,E10.0)
0096          IS=IS+1
0097          GO TO (35,2,3,3),IS
0098    2     TCE=-TCE
0099          GO TO 35
0100    3     WRITE (2,1041) I
0101    1041  FORMAT (/"DVM OVERLOAD AT DATA POINT",I4)
0102          CALL DVS (V(I))
0103          GO TO 40
0104    35    CE(I)=CE(I)+TCE
0105          IF (10.-ABS(CE(I))) 1,4
0106    1     NCODE=3
0107          WRITE (10) NCODE
0108    4     CE(I)=CE(I)/GAIN
0109          CALL RDPS (IERR)
0110          IF (IERR-1) 30,8
0111    8     WRITE (2,1045) I
0112    1045  FORMAT (/"DVS ERROR AT DATA POINT",I4)
0113          GO TO 40
0114    30    CONTINUE
0115          CALL DVS (V(I))
0116    5     CALL SWR(0,ID)
0117          IF (ID) 7,9
0118    7     CALL PPLOT (V,CE,NW)
0119          CALL SWR(0,ID)
```

```
0120          IF (ID) 40,9
0121    9     IFL=1
0122          DO 60 I=2,NW
0123          IF (ABS(CE(I))-ABS(CE(IFL))) 11,60
0124    11    IFL=I
0125    60    CONTINUE
0126          CPF=CE(IFL)
0127          VPF1=V(IFL)
0128          CALL DVS (VPF1)
0129          DO 70 I=1,NW
0130    70    V(I)=V(I)-VPF1
0131          DVIS=VIS/DV
0132          IDV=DVIS
0133          IF (IDV-3) 12,13
0134    12    IDV=3
0135    13    IF (IFL-(IDV+1)) 14,15
0136    14    WRITE (2,1060)
0137    1060  FORMAT ("V(MIN) TO VIS INCLUDES V(IFL)")
0138          GO TO 10
0139    15    CALL LILSQ (V(1),CE(1),IDV,D,ER1,ER2)
0140          SL=D(1)
0141          CPO=D(2)
0142          VPC=-CPO/SL
0143          WRITE (2,1070) DVIS,SL,CPO,ER1,ER2,VPC
0144    1070  FORMAT (//"ION CURRENT APPROXIMATION (",F5.1," INCREMEN
0145         *TS)"/2X,"CI =",E10.4," + V +",E11.4,4X,"EMAX =",E10.4,
0146         *3X,"ERMS =",E10.4/2X,"ZERO ION CURRENT AT",F6.2," VOLTS";
0147          IMAX=IFL-1
0148          DO 80 I=IDV,IMAX
0149          J=IFL-I
0150          CIC=0.99*(CPO+SL*V(J))
0151          IF (CIC-CE(J)) 80,21
0152    80    CONTINUE
0153          WRITE (2,1080)
0154    1080  FORMAT (/"STRAIGHT LINE APROX NOT VALID")
0155          GO TO 10
0156    21    NI=J
0157          DO 90 I=NI,NW
0158          IF (V(I)-VPC) 17,18
0159    17    TS(I)=CE(I)-(CPO+SL*V(I))
0160    18    IF (TS(I)-0.01) 19,90
0161    19    TS(I)=0.01
0162    90    CONTINUE
0163          INC=NUL-1
0164          NN1=NI+INC
0165          NN2=NW-INC
0166          DO 110 I=NN1,NN2
0167          S1=A(1)*TS(I)
0168          DO 100 J=1,INC
0169          K=J+1
0170          IP=I+J
0171          IM=I-J
0172          SUM=TS(IM)+TS(IP)
0173    100   S1=S1+A(K)*SUM
0174          IF (S1-0.01) 101,102
0175    101   S1=0.01
0176    102   CES(I)=S1
0177    110   ALCES(I)=ALOG(S1)
0178          NN3=NN1+INC
0179          NN4=NN2-INC
```

```
0180          DO 130 I=MM3,MM4
0181          S2=0.
0182          S3=C(1)*CES(I)
0183          DO 120 J=1,INC
0184          K=J+1
0185          IP=I+J
0186          IM=I-J
0187          S2=S2+B(K)*(ALCES(IP)-ALCES(IM))
0188   120    S3=S3+C(K)*(CES(IM)+CES(IP))
0189          S2=S2/DV
0190          IF (-S2) 121,122
0191   122    S2=100.*E/XK
0192   121    TS(I)=E/(S2*XK)
0193          S3=S3/(DV*DV)
0194   130    SDCES(I)=S3
0195          MM4A=MM4-5
0196          DO 140 I=IFL,MM4A
0197          IF (SDCES(I)) 131,140
0198   131    IF (SDCES(I+5)) 132,140
0199   132    ISP=I
0200          IF (SDCES(I-1)+SDCES(I)) 133,150
0201   133    ISP=ISP-1
0202          GO TO 150
0203   140    CONTINUE
0204          ISP=IFL
0205          WRITE (2,1200)
0206   1200   FORMAT ("DATA DOES NOT EXTEND TO PLASMA POTENTIAL")
0207   150    CONTINUE
0208          WRITE (2,1090)
0209   1090   FORMAT (/6X,"INDEX",7X,"V",12X,"CP",10X,"CES")
0210          WRITE (2,1100) V(1),CE(1)
0211   1100   FORMAT ("MIN",6X,"1",1X,2E13.4)
0212          WRITE (2,1110) MI,V(MI),CE(MI)
0213   1110   FORMAT ("MI",I6,1X,2E13.4)
0214          WRITE (2,1120) MM1,V(MM1),CE(MM1),CES(MM1)
0215   1120   FORMAT ("MM1",I7,1X,3E13.4)
0216          WRITE (2,1130) MM3,V(MM3),CE(MM3),CES(MM3)
0217   1130   FORMAT ("MM3",I7,1X,3E13.4)
0218          WRITE (2,1140) IFL,V(IFL),CE(IFL),CES(IFL)
0219   1140   FORMAT ("IFL",I7,1X,3E13.4)
0220          WRITE (2,1150) ISP,V(ISP),CE(ISP),CES(ISP)
0221   1150   FORMAT ("ISP",I7,1X,3E13.4)
0222          WRITE (2,1160) MM4,V(MM4),CE(MM4),CES(MM4)
0223   1160   FORMAT ("MM4",I7,1X,3E13.4)
0224          WRITE (2,1170) MM2,V(MM2),CE(MM2),CES(MM2)
0225   1170   FORMAT ("MM2",I7,1X,3E13.4)
0226          WRITE (2,1180) NE,V(NE),CE(NE)
0227   1180   FORMAT ("MAX",I7,1X,2E13.4)
0228          DVFP=VFP/DV
0229          IDV=DVFP
0230          IF (IDV-3) 151,152
0231   151    IDV=3
0232   152    MST=IFL+IDV
0233          CALL LILSQ (V(MST),ALCES(MST),IDV,D,ER1,ER2)
0234          IF (-D(1)) 153,154
0235   154    D(1)=100.*E/XK
0236   153    TES=E/(XK*D(1))
0237          WRITE (2,1190) TES,ER1,ER2
0238   1190   FORMAT (/"TE AT V(IFL) =",F7.0," DEG K",5X,"EMAX =",E10
0239         *.4,3X,"ERMS =",E10.4)
```

```
0240          VDL=V(ISP)*D(1)
0241          CI=-(CP0+SL*V(IFL))
0242          DENS2=0.
0243          DEN2A=0.
0244          DENS4=0.
0245          DENS1=CI*SQRT(XM*XMP/(XK*TES))*1.E-12/(1.13*E*PI*R*XL)
0246          DVSC=10.0/DV
0247          IDV=DVSC
0248          ICB=IFL-IDV
0249          IF (-ICB) 156,155
0250   155    ICB=1
0251   156    CP=CE(ICB)
0252          IF (ICB-MI) 172,171
0253   171    CP=CP0+SL*V(ICB)
0254   172    IF (CP) 157,158,157
0255   157    VPICB=ABS(V(ISP)-V(ICB))
0256          IF (ISP-IFL) 159,160,159
0257   160    VPICB=VPICB+5.*TES*XK/E
0258   159    DVSC=VPICB/DV
0259          DELA=SQRT(E*(2.*VPICB)**3/(XM*XMP))
0260          DELB=4.*PI*EPS*XL/(9.*R*CP+1.E-6)
0261          DELC=SQRT(E*VPICB/(XK*TES))
0262          BETA2=ABS(DELA*DELB*(1.+2.66/DELC))
0263          IF (0.5-BETA2) 161,162
0264   162    DELS=R*(9.5547E-2*BETA2+1.001*SQRT(BETA2)-5.7212E-5)
0265          GO TO 165
0266   161    IF (5.0-BETA2) 163,164
0267   164    DELS=R*(7.81E-2*BETA2+1.0315*SQRT(BETA2)-1.388E-2)
0268          GO TO 165
0269   163    DELS=R*(6.884E-2*BETA2+1.0791*SQRT(BETA2)-7.413SE-2)
0270   165    RS=R+DELS
0271          XS=XL+DELS
0272          RD=R/RS
0273          WRITE (2,2001) VPICB,DVSC,BETA2,DELS,RS,XS,RD
0274   2001   FORMAT (/"SHEATH CALCULATIONS"/5X,F5.2," VOLTS BELOW
0275         *V(ISP) (",F5.1," INCREMENTS)"/5X,"BETA2 =",E10.4/5X,"
0276         *SHEATH THICKNESS =",E10.4/5X,"RADIUS =",E10.4," METERS
0277         *"/5X,"LENGTH =",E10.4," METERS"/5X,"RP/RS =",E10.4)
0278          IF (14.-BETA2) 166,167
0279   167    DENS4=-(CP*SQRT(XM*XMP/(XK*TES))*1.E-12)/(1.13*E*
0280         *PI*RS*XS)
0281   168    WRITE (2,1210) DENS1,DENS4
0282   1210   FORMAT (/"ION NUMBER DENSITY ="/5X,E11.5," AT V(IFL)"/
0283         *5X,E11.5," AT V(IFL)-10 (USING SHEATH)")
0284   158    CONTINUE
0285          BK=XK*1.E7
0286          RP=R*100.
0287          EV=XK*TES/E
0288          CGE=4.8022E-10
0289          WRITE (2,501)
0290   501    FORMAT (/3X,"DEB",4X,"TI/TE",4X,"RP/LD",5X,"VPF",5X,
0291         *"DENSITY")
0292          RT=SQRT(XMI/(XM*XMP))
0293          DEB1=SQRT(BK*TES/(4.*PI*CGE*CGE*DENS1))
0294          JP=0
0295          VLT=10.0
0296   299    JPASS=0
0297          DEB=DEB1
0298          RPLD=RP/DEB
```

```
0300  300   GO TO (301,303,310),JP
0301  301   ITITE=1
0302        CII=2.E-4*RPLD*RPLD-0.031752*RPLD+2.8366
0303        GO TO 305
0304  303   ITITE=0
0305        CII=1.6E-4*RPLD*RPLD-0.02848*RPLD+2.2570
0306  305   VPN=-ALOG(RT*CII)
0307        VPF=VPN*EV
0308        IVS=IFL+IFIX(VPF/DV)
0309        IVN=VLT*EV/DV
0310        IVI=IVS-IVN
0311        VIVI=V(IVI)
0312        IF (-IVI) 307,306
0313  306   VIVI=V(1)+FLOAT(IVI-1)*DV
0314  307   CPP=CPO+SL*VIVI
0315        DENS3=-CPP*SQRT(XM*XMP/(2.*PI*XK*TES))*1.E-12/(CII*R*XL*E)
0316        DEB3=SQRT(BK*TES/(4.*PI*CGE*CGE*DENS3))
0317        DEBD=ABS(DEB-DEB3)
0318        IF (DEBD-0.01*DEB1) 309,314
0319  314   DEB=DEB3
0320        RPLD=RP/DEB
0321        JPASS=JPASS+1
0322        IF (9-JPASS) 309,300
0323  309   WRITE (2,502) DEB3,ITITE,RPLD,VPF,DENS3
0324  502   FORMAT (ES.3,I5,E12.3,F8.2,E11.3)
0325        IF (9-JPASS) 311,299
0326  311   WRITE (2,500) DEBD
0327  500   FORMAT ("**DEBD =",F6.4)
0328        GO TO 299
0329  310   CONTINUE
0330        PAUSE 4
0331        CALL SWR (1,ID)
0332        IF (ID) 22,23
0333  22    N=ISP-XM3+5
0334        CALL PPLOT (V(XM3),TS(XM3),N)
0335  23    CALL SWR (2,ID)
0336        IF (ID) 24,26
0337  24    WRITE (4,1050) NUM1A,NUM1B,NUM2,CM,TES,VFP1,V(IVS),DENS3
0338       *,DENS4
0339  1050  FORMAT (3I3,6E10.4)
0340  26    CONTINUE
0341        GO TO 10
0342        END
0343        END$
```



```
**END-OF-TAPE
*
/E
```

Vita

Victor Robert Trouy was born on 13 September 1936 in Helena, Arkansas. He received the degree of Bachelor of Science in physics from Christian Brothers College in Memphis, Tennessee in 1962. He was commissioned a Lieutenant in the Air Force upon completion of Officers Training School in 1962. He received the aeronautical rating of pilot in 1965, and served flying tours in Hawaii, Southeast Asia and Florida.

Permanent Address: 1863 Lorrie Lane
Memphis, Tennessee